The Journal of Experimental Biology 211, 2989-3000
Published by The Company of Biologists 2008
doi:10.1242/jeb.014357

Running on uneven ground: leg adjustment to vertical steps and self-stability

Sten Grimmer[1,*], Michael Ernst[1], Michael Günther[1,2] and Reinhard Blickhan[1]

[1]Friedrich-Schiller-Universität, Institut für Sportwissenschaft, Lehrstuhl für Bewegungswissenschaft, Seidelstraße 20, D-07749 Jena, Germany and [2]Eberhard-Karls-Universität, Institut für Sportwissenschaft, Arbeitsbereich III, Wilhelmstraße 124, D-72074 Tübingen, Germany

*Author for correspondence (e-mail: sten.grimmer@uni-jena.de)

Accepted 11 June 2008

SUMMARY

Human running is characterized by comparably simple whole-body dynamics. These dynamics can be modelled with a point mass bouncing on a spring leg. Theoretical studies using such spring–mass models predict that running can be self-stable. In simulations, this self-stability allows for running on uneven ground without paying attention to the ground irregularities. Whether humans actually use this property of the mechanical system in such an irregular environment is, however, unclear. One way to approach this question is to study how the leg stiffness in stance and the leg orientation in flight are changed in response to ground perturbations. Here, for 11 human subjects we studied two consecutive contacts during running on uneven ground with a force plate of adjustable height (step of +5, +10 and +15 cm). We found that runners adjust their leg stiffness to the height of a vertical step. The adjustment is characterized by a 9% increase in leg stiffness in preparation for the perturbation and by a systematic decrease in proportion to the step height. At the highest vertical step (+15 cm), leg stiffness was reduced by about 26%. We also observed that the angle of attack decreased from 68 deg. to 62 deg. with increasing ground height. These leg adjustments are in accordance with the predictions of a stable spring–mass system. Furthermore, we could describe the identified leg forces and leg compressions with a simple spring–mass simulation for a given body mass, leg stiffness, angle of attack and initial conditions. We compared the experimental findings with the self-stabilizing properties of the spring–mass model, and discuss how humans use a combination of strategies that include purely mechanical self-stabilization and active neuromuscular control. Finally, beyond self-stability, we suggest that control may apply to smooth centre of mass kinematics.

Key words: biomechanics, human locomotion, spring–mass model, leg stiffness, self-stability.

INTRODUCTION

When humans run they have to face all kinds of terrain: streets made of asphalt and limited by kerbs, or nature trails and pathways covered with stones, grass and roots. It seems that human runners have few problems dealing with all these irregularities. Recent investigations have shown that running performance on uneven ground may rest on carefully adjusted leg mechanics (Schmitt et al., 2002; Blickhan et al., 2003; Blickhan et al., 2007).

A simple approach to describe the basic mechanics of human locomotion is the spring–mass model (Blickhan, 1989). Since its introduction it has been used in several research studies of hopping and running (e.g. Farley et al., 1991; Blickhan and Full, 1993; Full and Koditschek, 1999; Seyfarth et al., 2002; Geyer et al., 2006; Seyfarth et al., 2006) and in recent investigations of walking (Geyer et al., 2006). The model consists of a mass-less spring and the body represented by a point mass and is simply described by the parameters stiffness k, angle of attack α_0 and leg length l_0 (Blickhan, 1989; McMahon and Cheng, 1990; Geyer, 2005). Stiffness was identified as the key parameter to describe the dynamics of running (Ferris et al., 1998). In several investigations the model was used to describe the dependence of stiffness on speed (McMahon and Cheng, 1990; Farley et al., 1993) and hopping or stride frequency (Farley et al., 1991; Farley and Gonzalez, 1996). Other experiments demonstrated an adjustment of leg stiffness to ground stiffness in hopping and running (Ferris and Farley, 1997; Farley et al., 1998; Ferris et al., 1998; Kerdok et al., 2002; Lindstedt, 2003; Moritz and Farley, 2004). All these studies on the interaction of the spring–mass model with ground compliance are based on two springs in series: one representing the leg and the other the ground (Alexander, 1997). The main result is that total stiffness (inverted sum of compliances) is rather constant and leg stiffness adapts to the ground stiffness by adjusting the leg compression (Ferris and Farley, 1997; Ferris et al., 1998). This leg behaviour might also be a possible strategy for varying ground levels but has not yet been reported in humans.

In an experimental observation on birds running over a track with an unexpected drop, it was shown that an adaptation of the angle of attack explains most of the variation in stance-phase dynamics (Daley and Biewener, 2006; Daley et al., 2006). Although stiffness varied dramatically it is not clear how this leg stiffness adjustment contributes to match the varying surface.

Recently, simulations and analytical calculations have provided evidence for self-stable operation of the spring–mass model for a limited range of combinations of the angle of attack and leg stiffness (Seyfarth et al., 2002; Geyer et al., 2005). Under these conditions the system is able to cope with uncertainties, such as uneven ground, without adjusting system properties, i.e. without directly sensing the disturbance. Self-stability was formulated as the underlying concept (Ringrose, 1997b; Wagner and Blickhan, 1999; Full et al., 2002; Blickhan et al., 2003; Blickhan et al., 2007). Here, neural feedback is not necessary. However, the mechanical ability depends on a well-adjusted angle of attack and leg stiffness (Seyfarth et al., 2002). Thus, on uneven terrain, using self-stability might require changing leg stiffness and angle of attack.

In part, this change can automatically be achieved by late swing leg retraction (Seyfarth et al., 2003). This rotational behaviour of the swing leg changes the angle of attack depending on the flight time

(the longer the flight phase, the steeper the angle of attack). Leg retraction greatly enlarges the range of leg stiffness and angle of attack that the model can tolerate. In simulations, by using leg retraction, changes in ground level of 50% of the initial leg spring length can be managed (Seyfarth et al., 2006). Although swing-leg retraction is an important stabilizing mechanism, it has limitations at higher speeds and cannot increase stability by increasing the rotational velocity (Seyfarth et al., 2003; Seyfarth et al., 2006). Here, alternative strategies might be crucial for stable running. However, for both 'running with fixed angle of attack' and 'running with leg retraction', the ability to cope with uneven terrain and the evidence of self-stability has been reported.

Recently, in a commentary, Biewener and Daley suggested integrative biomechanical approaches, i.e. a combination of modelling and experimental techniques, to understand locomotion over a variety of conditions (Biewener and Daley, 2007). Such approaches need to investigate the elegant interplay of intrinsic mechanisms (e.g. self-stability) to achieve stability and strategies of changing parameters in an appropriate way to the environment to achieve agility.

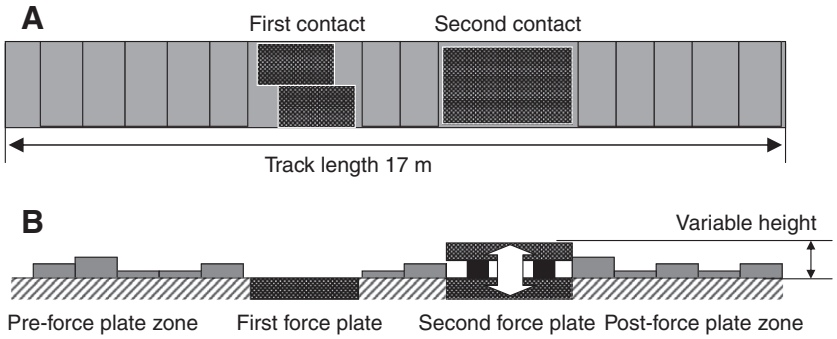

Fig. 1. The running track setup near the force plates. (A) View from above. The track is instrumented with two force plate sections. The first one (first contact) consists of two small Kistler force plates (Kistler 9282BA, size 600 mm×400 mm) and the second (second contact) of one large Kistler force plate (Kistler 9285C, size 900 mm×600 mm). (B) View from the side. Before, between and after the force plates the track is uneven (vertical perturbation between 1 and 2.5 cm). These small perturbations are made with wooden bars (width 120 mm). Note that in this sketch the ratio between the width of the bars and the length of the force plates is exaggerated for clarity. The first force plate represents ground level of vertical height zero. The second force plate acts as a single perturbation (step), which is variable in vertical height. Four track conditions were measured: level track (no perturbation at all) and an uneven track, i.e. varying height of bars before and after the force plates plus vertical steps of 5, 10 and 15 cm onto the second force plate.

In this investigation, we focused on leg adjustments on uneven ground and how they are linked to the concept of self-stability. We addressed two main research questions. (1) Do humans use a control strategy mainly explained by a stiffness adjustment process? (2) Does the adjustment utilize the self-stability of the underlying mechanical system and, thus, is the adjustment of the angle of attack and a proper stiffness as predicted by the spring–mass simulations the key feature for stable running on varying ground?

MATERIALS AND METHODS

The investigation was divided into two parts. In the first part, we observed human running on an uneven track with a perturbation consisting of a force plate varying in height. From the measured kinematics and kinetics we calculated the leg behaviour during the stance phase. In the second part, we compared these results with a simulation using a spring–mass model.

The experiment on uneven ground

Running track and setup

A 17 m long track was instrumented with three force plates. Two smaller ones (9282BA, Kistler, Winterthur, Switzerland) were mounted side by side and displaced 20 cm (Fig. 1A). A larger one (9285C, Kistler) was added at a distance of one step. Both force plates could be hit with step lengths from 1.60 to 2.50 m. In addition, the second plate was adjustable in height (Fig. 1B). We used the plate as an obstacle on the track.

A flat and an uneven track were introduced. We measured the flat track as a reference for our subsequent experimental conditions. For the uneven track we changed the height of the second force plate to 5, 10 and 15 cm (note that the first two force plates were kept in their vertical position). In front of and behind the plates the track was rough, consisting of wooden bars (width of 120 mm) with heights varying randomly between 10 and 25 mm. The bars were adjoined seamlessly and arranged crosswise to the running direction. Due to these bars, a small step down to the first contact plate was introduced. The height of this step down varied depending on the placement of the foot on the track. Track and force plates were covered with a 10 mm tartan layer to smooth the edges of the bars.

We used a twelve camera 3D motion capture system (240 Hz, 658 pixels×496 pixels; Qualisys, Gothenburg, Sweden) to measure the kinematics. A rough estimate of the spatial resolution was made by determining the noise level of the coordinates of a static marker. We found a resolution of about ±0.3 mm (about factor 10 subpixel resolution). The subject's body was marked (marker size 18 mm) on the hips, knees, ankles and balls of the feet (Fig. 2) as well as on the head and vertebra T1. The head and T1 markers were only used to obtain running speed, which was provided to the subjects.

Subjects

We studied 11 male subjects (all active runners: mean mass 74.1±9.8 kg, mean height 1.80±0.05 m) running on the track. The athletes were all sports students and had a high performance level in their sport. We chose such a homogeneous group because we aimed to have subjects with a robust running technique, i.e. the ability to run at a uniform speed. Moreover, in order to enable comparison with the simulation results, a minimum speed of 3.5 m s^{-1} was required (Seyfarth et al., 2002).

Subjects were informed about the risks of tripping and falling due to the experimental design. They provided written informed consent prior to their participation. The investigation was approved by the ethics review board of the University of Jena and the experiments were conducted in accordance with the Declaration of Helsinki.

Experimental protocol

After introducing the subjects to the track we started a running sequence without any perturbation. This procedure enabled us to check all measurement systems, gave a good warm up, and trained the subjects to maintain their velocity. A subject began running in the pre-force plate zone, then came into contact with the ground-level force plate (first contact). In the stride that followed the first force plate, the subject contacted a variable height force plate (second contact). Afterwards, the subject continued running into the post-

force plate zone, ending the trial. At the end of each trial the subject was instructed to decelerate, turn around and slowly jog back to the beginning of the running track. While jogging back, the investigator made a quick decision based on the horizontal velocity of the T1 marker (available online) to delete trials with obvious acceleration between the penultimate step before the first force plate and the first step after the second force plate.

The experimental investigation started with subjects running on the flat track. Afterwards, we prepared the uneven track. We then began taking measurements from trials on the uneven track with the 5, 10 and 15 cm perturbation. The subjects were visually aware of the whole running track and were allowed to get familiar with each height of the perturbation through one or two initial trials. In each of the four track conditions the subject had to accomplish at least 15 trials in a row.

Data processing

From the collected data, we filtered out all those trials of each subject that were distributed in a preferably narrow range from their preferred running speed over all track types. The selection was realized in three stages. First, we calculated the mean of the horizontal velocity of the T1 marker for each force plate. If these two values differed by more than 5% within one trial then this trial was discarded. Next, we calculated a mean overall remaining speed for both force plates and all track types for each subject. In the last stage, we further discarded all those trials where speed differed by more than 5% from this overall subject mean. After these selection steps we had on average 10 trials per experimental condition and subject (minimum three, maximum 15 trials).

The raw kinematic data were preprocessed to guarantee constant segment lengths (Günther et al., 2003) and filtered with a fourth-order low-pass Butterworth filter (Winter, 2005) at 20 Hz cut-off frequency.

The distance between the hip and ball of the foot marker is defined as leg length l_{leg} of the stance leg. The leg stiffness k_{leg} was calculated as the ratio between the peak ground reaction force F_{max} and the maximum leg compression $\Delta l_{leg,max}=l_{leg,TD}-\min.(l_{leg,TD:TO})$ (where TD is touch-down and TO is take-off) (McMahon and Cheng, 1990; Seyfarth, 2000):

$$k_{leg} = \frac{F_{max}}{\Delta l_{leg,max}} . \quad (1)$$

To compare the results of each subject we used all parameters in dimensionless form (Blickhan, 1989; Geyer, 2005). The leg force was normalized to subject mass m and gravity constant g:

$$\tilde{F} = \frac{F}{mg} \quad (2)$$

with the body weight bw=mg. The leg length was normalized to the initial leg length:

$$\tilde{l}_{leg} = \frac{l_{leg}}{l_0} , \quad (3)$$

with:

$$\Delta\tilde{l}_{leg} = 1 - \tilde{l}_{leg} . \quad (4)$$

Therefore, the dimensionless stiffness according to Eqns 1–3 is:

$$\tilde{k}_{leg} = \frac{\tilde{F}_{max}}{\Delta\tilde{l}_{max}} . \quad (5)$$

To compare the different track conditions with the three heights of the force plate (i=1,2,3) and the 11 subjects, we also normalized each parameter ($\tilde{k}_{leg}$, $\tilde{F}_{max}$, $\Delta\tilde{l}_{leg,max}$) to a subject-specific reference mean value. This mean value was extracted from normal running without perturbations (track type i=0).

Statistics

We present the results of the investigation as descriptive statistics (parameter values in tables with means ± s.d.) over all subjects and parameters. An inferential statistic is only used for the mean-normalized global parameters (stiffness, force and compression) to show the significant change within the flight phase of the consecutive contacts. For this purpose, we used a Friedman test for paired observations (Friedman, 1937; Friedman, 1939; Siegel and Castellan, 1988). The statistics were processed with the statistical toolbox of Matlab (release 14, Mathworks Inc., Natick, MA, USA).

Model and simulation

Model

Our simulation consisted of a conservative spring–mass model. The elastic stance phase was modelled with a point mass attached to a mass-less linear spring (Blickhan, 1989) and the flight phase was a simple ballistic behaviour of the point mass with a reset of the leg angle to the angle of attack at TD (Seyfarth et al., 2002). We simulated two consecutive contacts in which in the second contact we varied the spring stiffness and angle of attack as well as the ground height.

Simulation parameter setup and analysis

The initial conditions for the first contact were about average values of the subjects: horizontal component of the initial velocity $v_{x,0}$=4.5 m s^{-1}, initial apex height y_0=0.95 m, body mass m=80 kg, initial leg length l_0=1 m, dimensionless stiffness $\tilde{k}$=35.7 (k=28 kN m^{-1}), and a fixed angle of attack of α_{TD}=68 deg., which is also typical for level running (Seyfarth et al., 2002).

In the second contact we introduced a disturbance with a ground height of +15 cm (equal to experimental track type i=3). Here, to

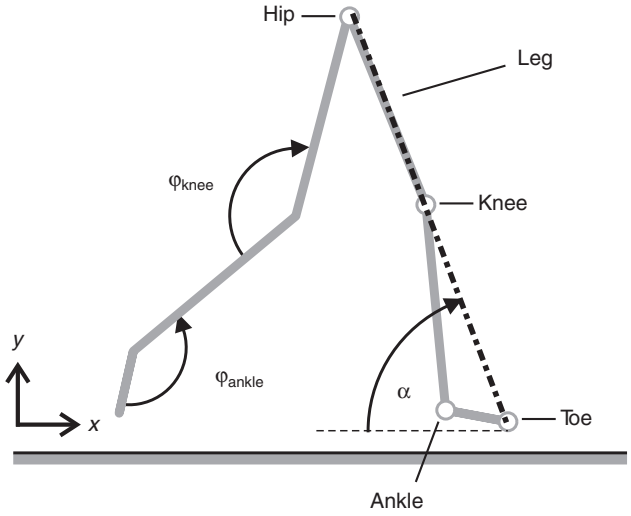

Fig. 2. The marker setup and angle definitions. Subjects were marked at the hip (trochanter major), knee, ankle and ball of the foot as well as on the head and the vertebra T1 (head and T1 markers are not shown in the sketch). We calculated the inner angles at the knee (φ_{knee}) and ankle (φ_{ankle}) joint. According to the spring–mass model, we defined the leg as the distance between the hip and toe marker. The leg angle (α) is measured clockwise with respect to the negative x-axis.

cover the experimental values, we mapped the peak spring force F_{max} and maximum spring compression $\Delta\tilde{l}_{max}$ for a range of angles of attack (α_{TD}=50:75 deg.) and spring stiffnesses ($\tilde{k}$=5:50).

Simulation tools

The model was built in Simulink, Matlab R14 (Mathworks Inc.) with a variable step-size integrator (ode45) and a relative tolerance of 1e–12. As part of the simulation the system energy was checked and remained constant over the simulation time (relation energy fluctuation <1e–10).

RESULTS

Experimental results

While running across an uneven track the quasi-elastic operation of the human leg was maintained (Fig. 3A,B). The leg was still compressed and stretched during stance phase. However, stiffness was adjusted (Fig. 3B). Leg stiffness defined as the ratio between peak force and maximum leg compression during ground contact decreases in proportion to the height of the step (Eqn 1, respectively Eqn 5). Comparing the reference run and the highest perturbation values, subjects increased leg stiffness in the first contact from 34.3±6.8 to 36.0±6.2 bw l_0^{-1} and decreased leg stiffness in the second contact from 32.5±4.8 to 23.7±4.4 bw l_0^{-1} (Table 1). While in the first contact there was only a small increase in leg stiffness (values in preparation for the subsequent contact for 0 cm: 34.3±6.8 bw l_0^{-1}; 5 cm: 36.7±6.6 bw l_0^{-1}; 10cm: 36.9±4.9 bw l_0^{-1}; 15 cm: 36.0±6.2 bw l_0^{-1}), in the second contact leg stiffness deceased in an inversely proportional relationship with the height of the vertical step (values for 0 cm: 32.5±4.8 bw l_0^{-1}; 5 cm: 32.9±6.7 bw l_0^{-1}; 10 cm: 26.7±4.0 bw l_0^{-1}; 15 cm: 23.7±4.4 bw l_0^{-1}). Despite individual differences in the strength of the dependency, all subjects showed a similar trend.

The change in stiffness becomes manifest in an adaptation of the ground reaction force (GRF; Fig. 3C,D). In the first contact peak GRF rose about 0.3 bw and in the second contact it diminished by about 0.7 bw at the highest vertical step (track type 3) with respect to the reference value (track type 0). In contrast, the maximum leg compression was maintained nearly constant in both contacts (Fig. 3E,F). Further, we observed a shorter leg at touch-down in the second contact (Fig. 3F). This phenomenon increased with the height of the step and was distributed between the knee and ankle joint (Fig. 4). The increased angular flexion was generally higher in the knee than in the ankle (Table 2).

Normalizing leg stiffness, leg compression and peak force to the individual undisturbed mean values (Fig. 5, Table 3), we identified an increase in leg stiffness of about +9% in the first contact and a decrease of about –26% for the highest step height (track type i=3) in the second contact. The peak GRF values varied correspondingly. For maximum leg compression the mean values differed between ±4% in the first contact and between ±8% in the second contact of

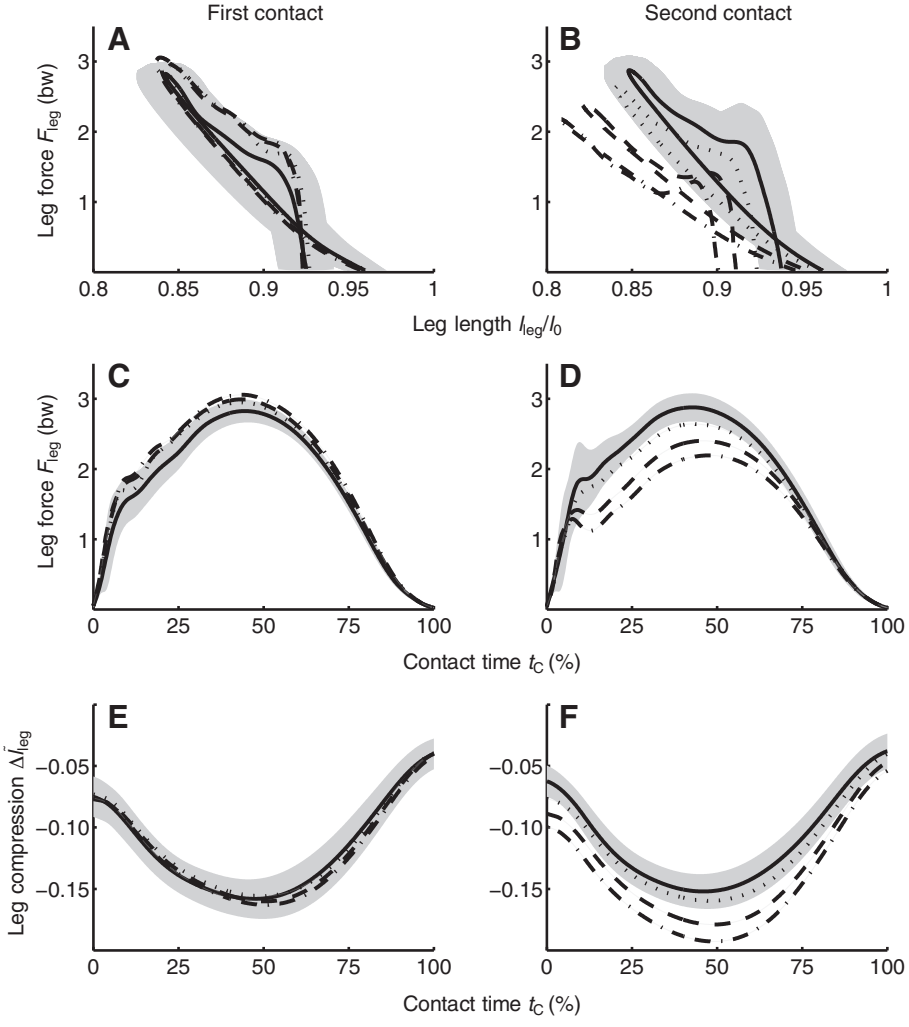

Fig. 3. Leg force and leg length during stance phase of the two subsequent contacts. The solid black lines represent level to level running (track type 0, N=99) and the grey shaded area is ±1 s.d. of this reference run on the undisturbed track, the dotted line from level to 5 cm up (track type 1, N=106), the dashed line from level to 10 cm up (track type 2, N=108) and the dashed-dotted line from level to 15 cm up (track type 3, N=110). (A,B) A quasi-elastic leg operation is observed in both contacts. However, the net energy balances are not zero (see Table 4). (C) The peak leg force is slightly increased in preparation for the consecutive step. (D) However, in the case of a perturbation the maximum leg force decreases in proportion to vertical step height. (E) The leg compression in the first contact is not affected in preparation for the vertical step. (F) Here, the leg length at initial contact (touch-down, TD) is shortened as well as the minimum leg length during contact in proportion to the vertical step height. Thus, leg compression remains almost constant.

Table 1. Parameters of global leg behaviour

	i	0	1	2	3
	Contact	0/0 cm	0/+5 cm	0/+10 cm	0/+15 cm
$\tilde{k}_{leg}$ (bw/l_0)	1	34.3±6.8	36.7±6.6	36.9±4.9	36.0±6.2
	2	32.5±4.8	32.9±6.7	26.7±4.0	23.7±4.4
$\tilde{F}_{max}$ (bw)	1	2.8±0.2	2.9±0.2	3.0±0.2	3.1±0.2
	2	2.9±0.2	2.6±0.2	2.4±0.2	2.2±0.2
$\Delta\tilde{l}_{leg,max}$ (l_0)	1	0.085±0.014	0.082±0.014	0.083±0.012	0.087±0.014
	2	0.091±0.011	0.083±0.015	0.091±0.012	0.095±0.014
$t_{\tilde{F}_{max}}$ (t_c)	1	0.446±0.024	0.424±0.034	0.431±0.033	0.441±0.032
	2	0.423±0.028	0.402±0.075	0.457±0.034	0.478±0.041
$t_{\Delta\tilde{l}_{leg,max}}$ (t_c)	1	0.475±0.038	0.492±0.034	0.505±0.032	0.510±0.030
	2	0.461±0.031	0.478±0.035	0.496±0.039	0.492±0.035
t_c (s)	1	0.194±0.022	0.192±0.024	0.196±0.026	0.198±0.024
	2	0.189±0.024	0.198±0.027	0.213±0.033	0.222±0.034
$\tilde{l}_{leg,TD}$ (l_0)	1	0.930±0.017	0.922±0.018	0.917±0.022	0.924±0.017
	2	0.939±0.013	0.916±0.017	0.910±0.013	0.901±0.016
$\tilde{l}_{leg,TO}$ (l_0)	1	0.963±0.015	0.956±0.011	0.953±0.013	0.958±0.013
	2	0.962±0.012	0.954±0.015	0.949±0.014	0.946±0.018
$\tilde{l}_{leg,shift}$ (l_0)	1	0.033±0.013	0.034±0.020	0.036±0.021	0.034±0.021
	2	0.023±0.015	0.038±0.020	0.040±0.019	0.045±0.019
α_{TD}(deg.)	1	68±2.6	69±2.5	68±2.6	67±2.5
	2	68±2.2	66±2.8	64±2.6	62±2.9
α_{TO}(deg.)	1	118±2.5	117±3.3	117±3.7	116±3.4
	2	117±2.2	118±2.3	119±3.0	121±3.0
α_{shift} (deg.)	1	50±3.1	49±3.7	49±3.7	49±3.3
	2	49±2.8	52±3.6	56±3.8	59±4.0
N		99	106	108	110

For descriptions of *i*, the different track types (0–3), see main text. For definitions see Table of abbreviations. Mean ± s.d. for all measured subjects separated for the two consecutive contacts. *N*: number of trials.

the undisturbed mean value. The mean value of maximum leg compression for undisturbed running in absolute units was about 9 cm (l_0=1.01±0.035 *m*). Our observed maximum deviation from the reference compression was about 8% (Table 3, $\Delta l_{leg,max,i=1}/\Delta l_{leg,max,i=0}$=0.92). This equals a fluctuation of leg compression of less than 1 cm during running over a perturbation of 15 cm.

Looking at the stride-to-stride analysis, we found that the stiffness of two subsequent contacts was equal on a track where the height of the force plate was 5 cm. Differences were found between subsequent contacts in the other track conditions with 10 and 15 cm height (*i*=2 and *i*=3, Table 3). The peak GRF values show a significant difference for all analysed track types. The maximum leg compression values remained constant except for the trials with the smallest disturbance (5 cm, track type 1).

For the angle of attack α_{TD} (i.e. leg angle at the beginning of contact) we also found adaptations to the different track types (Table 1). The angle of attack varied in the first contact by about ±1 deg. and diminished in the second from 68 to 62 deg. with the increasing vertical height of the perturbation.

Fig. 6 presents the relationship of leg stiffness and angle of attack for a simulation based on the spring–mass model for running. The black J-shaped region represents combinations of angle of attack and leg stiffness with stable solutions of periodic movement patterns. While parameter combinations left of the black area still allow at least one more contact, not a single step is possible at the right side (simulation stops). The circles (first contact) and squares (second contact: track types 1–3) illustrate measured combinations for a typical subject with identical initial conditions used in the simulation. For both contacts the combinations of angle of attack and stiffness fall in areas where on level ground usually more than five steps are possible without further adjustment (Fig. 6). Interestingly, all experimentally measured combinations are located on the left side of the J-shaped stability boundary. However, only some combinations fall into the self-stable black area. Furthermore, a wider range of combinations of angle of attack (from 66 to 55 deg.) and leg stiffness (from 35 to 15) in the second contact is applied. Interestingly, two separate distributions of the two contacts can be identified. In the second contact flatter angles of attack as well as smaller leg stiffness values are prevalent.

Model predictions

Under the initial conditions and variations of spring stiffness and angle of attack listed in Materials and methods, the spring–mass system was able to cope with disturbances up to 15 cm, i.e. a successful contact with a subsequent flight phase could be simulated. Due to the fact that spring stiffness and angle of attack in the first contact were simulated with a fixed value pair (α_{TD}, $\tilde{k}$), the peak spring force and maximum spring compression result in unique values. In our case, the peak spring force was approximately F_{max}=3.5 bw and the maximum spring compression $\Delta\tilde{l}_{max}$=0.1.

For the second contact, we first demonstrate the effect that in principle emerges from single parameter variation (see ‘Stiffness variation’ and ‘Angle of attack variation’ below). Here, we simply compared each of the three different values of spring stiffness and angle of attack estimated from the experimental results. Second, we systematically present the peak spring force and maximum spring compression for an expanded range of spring stiffness and angle of attack (see ‘Stiffness variation and angle of attack variation’ below).

Stiffness variation

By using a fixed angle of attack of 61 deg. and decreasing the dimensionless spring stiffness from 25.5 to 19.1 to 12.7, the peak spring force decreased too (Fig. 7A). At the same time, the maximum

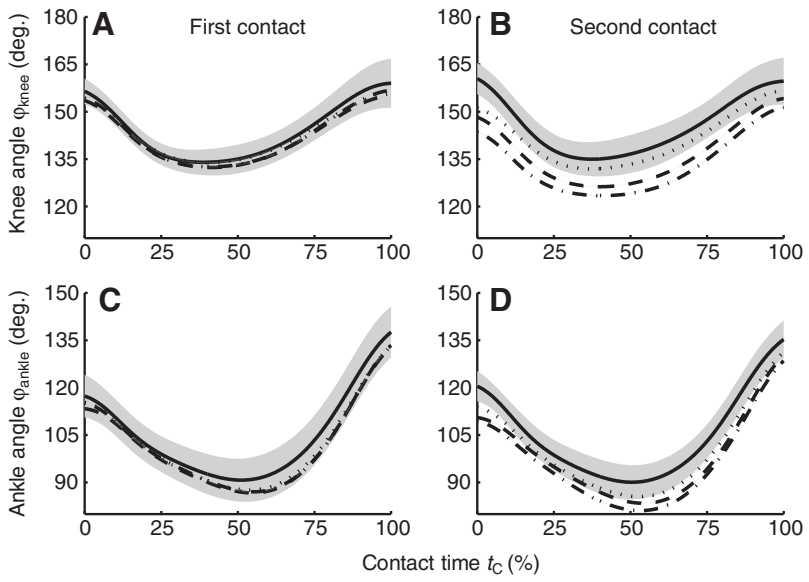

Fig. 4. Knee (φ_{knee}) and ankle (φ_{ankle}) joint angles during the two subsequent stance phases. (A,C) Both knee and ankle do not adapt in preparation for the following step as the mean values are within the mean area ±1 s.d. of the reference run. (B,D) Both adapt in the disturbed second contact as the initial contact joint angle ($\varphi_{knee,TD}$, $\varphi_{ankle,TD}$) as well as the minimum joint angle ($\varphi_{knee,min}$, $\varphi_{ankle,min}$) decrease. For detailed values see Table 2.

spring compression increased (Fig. 7C). Furthermore, maximum spring compression in the second contact was always larger than in the first contact.

Angle of attack variation

The variation in angle of attack compared with the variation in spring stiffness showed similar behaviour in the GRFs but different behaviour in spring compression. Here, by increasing the angle of attack from 59 to 61 to 63 deg. and using a constant dimensionless spring stiffness of 19.1, both the GRF and the spring compression decreased (Fig. 7B,D).

Stiffness and angle of attack variation

As shown in Fig. 8, by varying both parameters (angle of attack and stiffness), the simulation provided spring forces of up to 10 bw and maximum spring compressions of up to 0.5 times initial leg length. It was found that the maximum leg compression decreased with increasing spring stiffness and a steepening angle of attack (Fig. 8B). Likewise, the peak spring force decreased with steepening angle of attack. In contrast to maximum leg compression, a diminishing stiffness was needed for a decrease in peak spring force (Fig. 8A).

For the chosen initial conditions, the simulations led to successful contacts for up to an angle of attack of α_{TD}=63.2 deg. Further, it is remarkable that a small area of simulated parameter combinations of stiffness and angle of attack correspond with the experimentally measured peak leg force of 1.5 to 3 bw and maximum leg compression of 0.1 to 0.15 times initial leg length (Fig. 8, arrows).

DISCUSSION

Control strategy by stiffness adjustment process?

Runners adjust leg stiffness to the vertical height of a disturbance. This leg stiffness adjustment corresponds to an altered leg force and an almost unaffected leg compression. These effects can be observed in the preparation (first), as well as in the disturbed (second) contact. We identified a small increase in leg force (Fig. 3C) in the first contact as an active strategy with the aim of a higher take-off velocity and a higher apex of the following flight phase. Subjects were aware of the perturbation and did not want to stumble. Patla and Rietdyk measured a similar effect for obstacle clearance (Patla and Rietdyk, 1993). Their subjects increased vertical velocity in preparation for the obstacle height. As a result they elevated the hip position. Accordingly, we found that the vertical TO velocity of the hip was increased (0 cm: 0.8±0.2 m s^{-1}; 15 cm: 1.1±0.2 m s^{-1}) with the

Table 2. Joint angles

	i Contact	0 0/0 cm	1 0/+5 cm	2 0/+10 cm	3 0/+15 cm
$\varphi_{knee,TD}$ (deg.)	1	157±6	154±6	153±8	155±5
	2	161±6	151±7	148±8	144±7
$\varphi_{knee,min}$ (deg.)	1	133±4	133±4	132±4	132±4
	2	134±6	131±5	126±5	123±5
$\varphi_{knee,TO}$ (deg.)	1	158±8	155±6	154±7	157±6
	2	159±8	156±8	153±7	151±6
$\varphi_{ankle,TD}$ (deg.)	1	118±7	115±7	113±8	115±8
	2	121±5	112±9	110±7	109±8
$\varphi_{ankle,min}$ (deg.)	1	91±7	87±5	86±6	87±7
	2	90±5	84±7	83±6	80±7
$\varphi_{ankle,TO}$ (deg.)	1	137±8	133±5	132±7	133±6
	2	135±7	130±7	129±7	128±9
N		99	106	108	110

For definitions see Table of abbreviations. Mean ± s.d. for all measured subjects separated for the two consecutive contacts. *N*: number of trials.

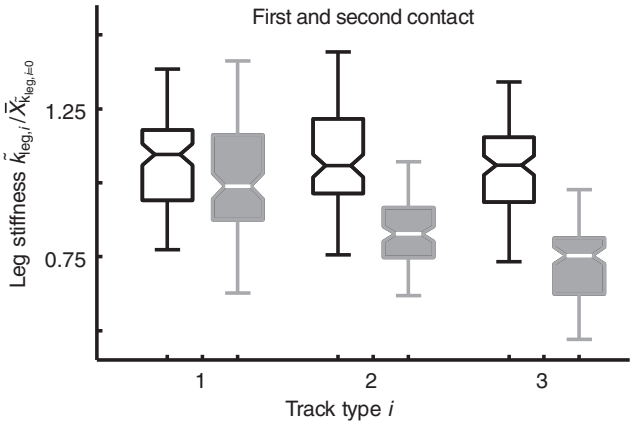

Fig. 5. Leg stiffness adaptation in the two consecutive contacts. We normalized each leg stiffness value for track types *i*=1–3 ($\tilde{k}_{leg,i}$) with a subject-specific reference run on the flat, undisturbed track ($\bar{X}_{\tilde{k}_{leg,i=0}}$) separately for each contact. Open boxes represent trials for the first contact, grey boxes those for the second contact. Leg stiffness was altered between contacts on bumpy ground (track type 1–3). Significant differences were found for track types 1, 2 and 3 (see Table 3).

subsequent height of the disturbance (Table 4, $v_{y,TO}$). Another possible effect is provoked by the longer flight phase caused by the uneven ground before hitting the first force plate. Higher landing velocities lead to higher GRFs (Cavanagh and Lafortune, 1980; Blickhan, 1989). We found that the vertical landing velocity of the hip was marginally increased (–0.6 *vs* –0.7 m s^{-1}) in the uneven track situations as it was on level ground (Table 4, $v_{y,TD}$). Yet, we do not know which effect dominates and the extent to which each effect corresponds to the increase in GRF.

In contrast to the first contact, our measured adaptations in the disturbed second contact are more striking and systematic. With increasing vertical height of the perturbation, leg force was decreased proportionally (Fig. 3D). This effect can be attributed to a lower vertical landing velocity (0 cm: –0.6±0.2 m s^{-1}; 15 cm: –0.1±0.1 m s^{-1}; Table 4, $v_{y,TD}$) caused by a reduced distance between the apex of the flight phase and the landing height at touch-down. The leg showed a tendency to be shorter at touch-down (Table 1, l_{TD}) but also to have a decreasing minimum length during contact at higher steps (Fig. 3D). As a result, leg compression remained constant. This effect may also rest on the initial conditions at touch-down and their effects on the muscle (Blickhan et al., 2007). According to the lever gear ratio of the two-segment leg (Wagner and Blickhan, 1999), also known as effective mechanical advantage (Biewener, 1989; Biewener et al., 2004), the load lever of the knee joint at touch-down increases when the knee is more flexed. The knee extensors are more elongated during contact and the effective mechanical advantage is reduced. In the case of nearly constant muscle force, the resulting leg force decreases. It is conceivable that both of these effects (reduced leg force and vertical landing velocity) may lead to an almost constant leg compression. Therefore, stiffness of the leg could be altered without sensory feedback as a response to the altered loading condition (landing velocity) and due to the changed working range of the muscles [force–length and force–velocity curve (e.g. Brown et al., 1996)].

Leg stiffness adjustment is well known in the case of running and hopping on ground varying with respect to compliance (Alexander, 1997; Ferris and Farley, 1997; Farley et al., 1998; Ferris et al., 1998; Ferris et al., 1999; Kerdok et al., 2002; Lindstedt, 2003). Ferris and colleagues reported in the case of stiffened ground that the leg response is characterized by a higher compliance, i.e. a lower stiffness (Ferris et al., 1997; Ferris et al., 1998). There, in contrast to our findings, the stiffer the ground the more the leg compression was increased, whereas the peak force was found to be rather constant. Therefore, the strategy on compliant ground is the direct opposite to that on uneven ground with vertical steps up.

Stiffness and angle of attack adjustment are explained by a simple spring–mass simulation

In spring–mass running, the simplest strategy is running with a fixed angle of attack and constant leg stiffness (Seyfarth et al., 2002). Here, with constant leg stiffness and subject-specific initial conditions, simulations revealed periodic movement patterns as well as an ability to cope with uncertainties such as rough terrain (Geyer et al., 2002). As mentioned earlier in our experiments, leg stiffness was altered. So, from a first point of view, the strategy of maintaining stiffness and angle of attack does not seem to apply. This is in contrast to the findings of Seyfarth and colleagues (Seyfarth et al., 2002). However, it has also been reported that there exists a range of solutions of leg stiffness adjusted to the angle of attack. By selecting one combination from the associated J-shaped area (Fig. 6), a spring–mass system can deliver self-stable cyclic movement (Seyfarth et al., 2002; Geyer et al., 2006). Yet, switching within this area can be read as a possible control strategy resulting in adapted leg stiffness due to an altered angle of attack. We found that angle of attack was altered. The higher the encountered step, the flatter the touch-down angle (Table 1). This would be expected for the case where the runner performs flight-phase retraction (Seyfarth et al., 2003). Flight-phase retraction automatically shifts the leg angle during flight, dependent on the flight-phase duration (de Wit et al., 2000; Günther and Blickhan, 2002; Daley and Biewener, 2006; Daley et al., 2006) without any control. Running

Table 3. Normalized global leg parameters

Parameter	*i*	*N*	First contact		Second contact		Significance	
$\tilde{k}_{leg,i}/\tilde{k}_{leg,0}$	1	106	1.09	±0.17	1.04	±0.25	0.007	**
	2	108	1.09	±0.17	0.84	±0.12	<0.001	**
	3	110	1.06	±0.17	0.74	±0.14	<0.001	**
$\tilde{F}_{max,i}/\tilde{F}_{max,0}$	1	106	1.05	±0.06	0.93	±0.04	<0.001	**
	2	108	1.07	±0.05	0.84	±0.04	<0.001	**
	3	110	1.08	±0.06	0.77	±0.04	<0.001	**
$\Delta\tilde{l}_{leg,max,i}/\Delta\tilde{l}_{leg,max,0}$	1	106	0.98	±0.14	0.92	±0.17	<0.001	**
	2	108	1.00	±0.14	1.01	±0.12	0.083	n.s.
	3	110	1.04	±0.15	1.07	±0.17	0.253	n.s.

For all other definitions see Table of abbreviations. Mean ± s.d. values of normalized leg stiffness, leg force and leg compression for all measured subjects separated for the two consecutive contacts. '**' indicate significant differences (Friedman-test, d.f.=1) $P<0.01$. n.s.: not significant, *N*: number of trials for each track type *i*. Table values belonging to Fig. 5.

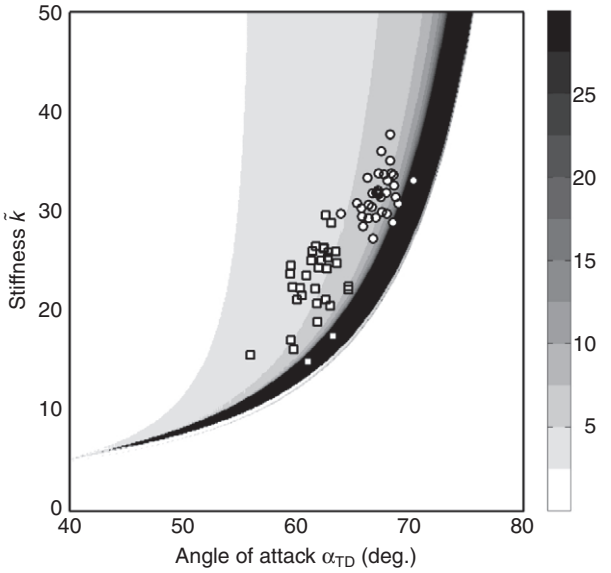

Fig. 6. Stability plot of a spring–mass simulation dependent on angle of attack (α_{TD}) and spring stiffness ($\tilde{k}$). Stable running requires a proper adjustment of angle of attack to spring stiffness (Seyfarth et al., 2002). The black J-shaped area guarantees at least 30 following contacts (end of simulation) and is referred to as the self-stable area. The circles (first contact) and squares (second contact) represent the data from the track types i=1–3 of a typical subject running at 4.8±0.16 m s^{-1}. Two distinct regions of stiffness and angle of attack combinations were found. From the first to the second contact both stiffness and angle of attack decrease in accordance with the results of the simulation. However, in most cases the experimental results do not fit into the area of self-stability but, rather, into an area that guarantees at least five subsequent contacts. Initial parameter of simulation: horizontal component of the initial velocity $v_{x,0}$=4.8 m s^{-1}, initial apex height y_0=1.0 m, body mass m=80 kg, initial leg length l_0=1 m. The grey scale on the right of the graph indicates how many subsequent steps of stable running can be made with the chosen combination of angle of attack and spring stiffness.

on uneven ground with a step up shortens the flight phase and decreases the angle of attack. Assuming that the change in leg stiffness is induced by the retracting leg being less extended at touch-down (see above), retraction can be identified as a key feature for shifting leg stiffness within the self-stable area.

As shown in Fig. 6, our experimental results fit these assumptions. As well as the first unaltered contact, the combinations also fit the altered disturbed second contact. Yet a shift from combinations of first to second contact in relation to the theoretical prediction is seen. However, not all experimental results fit to the area of self-stability. Most combinations allow at least five subsequent steps. This indicates that subjects chose not self-stable combinations but rather combinations that would allow for immediate stability, knowing that other mechanisms for stable control would engage in later stages of locomotion. The retraction control scheme may be one such type of control mechanism (Seyfarth et al., 2003; Seyfarth et al., 2006).

Force and compression can be predicted by a simple spring–mass simulation

As we found that leg stiffness and angle of attack are altered, we now examine the possible explanations for describing the dependency of the resulting parameters (peak force and maximum compression) within the spring–mass model. We found that a simple spring–mass simulation can produce the same force and compression parameters in the case of a 15 cm perturbation (area marked with arrows in Fig. 8) as those measured.

Furthermore, in simulations we found that for this region (arrows in Fig. 8), angles of attack between 61 and 63.2 deg. were in accordance with the experimentally observed angle of attack of 62±2.9 deg. The 63.2 deg. border in the simulation is due to the fact that the apex height is not high enough to match the landing height. By using a steeper angle of attack, the simulation stops because of stumbling. It is clear that changing the leg length at touch-down as observed in our experiment makes steeper angles of attack possible.

From the simulation results seen in Fig. 8, we derive two main outcomes of an alteration in stiffness. First, stiffness adaptation results in a nearly constant leg force and alteration of leg compression, which is found on compliant ground (e.g. Ferris et al., 1998; Ferris et al., 1999; Kerdok et al., 2002). Second, an altered leg force and constant leg compression can be caused by alterations of stiffness. This is generally what we found for running on steps of different heights. These two cases are limit cases for two different constraints (experimental conditions) perhaps due to the same additional movement criterion (smooth ride, see below). Deviations from these limit cases, i.e. a mixture of altered leg compression and leg force, can occur individually and are within the range of stable solutions predicted by the model. These deviations are caused by respective leg stiffness (experimental s.d.: ±6 bw l_0^{-1}) and angle of attack (experimental s.d.: ±2.5 deg.) variations.

The conservative spring–mass model and real energy losses

In contrast to the underlying spring–mass model, the legs of human runners show non-conservative work-loops (Fig. 3A,B, Table 4). In order to assess the consequences of net work balances on the validity of the spring–mass model, we estimated the influence of energy dissipation on the eigenfrequency of the model.

Geyer and colleagues provided an analytical solution for the equation of motion of the axial oscillation of a spring–mass model for running (Geyer et al., 2005). Therefore, two further approximations are needed: (i) leg compression is clearly smaller than leg length ($\Delta l/l_0 \ll 1$), and (ii) leg angle only marginally deviates from the vertical ($\sin(\alpha)\approx 1$). According to this model approach, the eigenfrequency of the conservative spring–mass model is $\omega_{SM}=\sqrt{(\omega_0^2+3\omega_p^2)}$ where $\omega_0=\sqrt{(k/m)}$ is the eigenfrequency of the harmonic oscillator made of the linear leg stiffness k (axial spring) and the body mass m, and $\omega_p=(mr^2\dot{\varphi})/(ml_0^2)\approx\dot{\varphi}\approx v_x/l_0$ is the contribution of the angular momentum of the body mass pivoting on the contact point of the spring. In humans, $\omega_0\approx\sqrt{(2\times10^4\,\mathrm{N\,m^{-1}}/70\,\mathrm{kg})}=16.9\,\mathrm{rad\,s^{-1}}$ dominates $\omega_{SM}=18.7\,\mathrm{rad\,s^{-1}}$ as $\omega_p=(4.5\,\mathrm{m\,s^{-1}}/1\mathrm{m})=4.5\,\mathrm{rad\,s^{-1}}$. Thus, we find that the angular momentum biases the oscillatory behaviour of bouncing locomotor dynamics (represented by ω_{SM}) by about 10% [(18.7–16.9)/16.9≈0.1].

The exact expression of the eigenfrequency $\omega_d(\omega_0,\Delta E_{leg}/E_{leg})$ of the damped harmonic oscillator (axial spring) in terms of its typical energy content $E_{leg}=\frac{1}{2}k_{leg}\Delta l_{leg,max}^2$ and net work balance:

$$\Delta E_{leg} = \int_{l_{TD}}^{l_{TO}} F\,\mathrm{d}l \qquad (6)$$

is given in the Appendix (see Eqn A6). Therefore, observing net work balances of $|\Delta E_{leg}/E_{leg}|=|-0.32\pm0.36|$ (Table 4), we find that ω_0 itself is biased by less than 1% for $|\Delta E_{leg}/E_{leg}|=0.5$ and by 3.5% for an extreme case $|\Delta E_{leg}/E_{leg}|=0.9$. Consequently, theory tells us that quasi-elastic leg operation is maintained even in the face of the measured net work balances.

Table 4. Velocity and energy balances

	i Contact	0 0/0 cm	1 0/+5 cm	2 0/+10 cm	3 0/+15 cm
$v_{x,TD}$ (m s^{-1})	1	4.4±0.4	4.3±0.5	4.3±0.5	4.3±0.5
	2	4.5±0.4	4.5±0.4	4.5±0.5	4.5±0.4
$v_{x,TO}$ (m s^{-1})	1	4.5±0.4	4.4±0.5	4.3±0.6	4.3±0.5
	2	4.5±0.4	4.6±0.4	4.5±0.5	4.6±0.5
$v_{y,TD}$ (m s^{-1})	1	–0.6±0.2	–0.7±0.2	–0.7±0.2	–0.7±0.2
	2	–0.6±0.2	–0.5±0.2	–0.3±0.2	–0.2±0.1
$v_{y,TO}$ (m s^{-1})	1	0.8±0.2	0.9±0.2	1.0±0.2	1.1±0.2
	2	0.8±0.2	0.8±0.2	0.7±0.2	0.6±0.2
ΔE_{leg} (J)	1	–8.0±22.3	–29.0±30.3	–34.1±35.0	–32.9±36.5
	2	–27.3±24.6	–15.2±19.8	–8.7±19.3	3.22±17.2
E_{leg} (J)	1	89.9±22.3	91.0±22.2	93.3±21.3	98.7±23.6
	2	98.5±23.9	81.6±20.3	81.9±19.0	76.7±16.2
$\Delta E_{leg}/E_{leg}$ (J)	1	–0.08±0.26	–0.28±0.31	–0.32±0.36	–0.29±0.35
	2	–0.28±0.28	–0.16±0.24	–0.09±0.25	0.05±0.25
N		99	106	108	110

For definitions see Table of abbreviations. Mean ± s.d. for all measured subjects separated for the two consecutive contacts. *N*: number of trials.

Self-stability and control

Our approach is also meant to verify whether the stiffness adaptations found may be an indicator of self-stability in human running. To address this, we simulated the self-stable movement of a mechanical model running across perturbations that matched the experimental conditions. A comparison of experimental and simulated adaptations answers the question whether running across uneven ground might be based on self-stability, i.e. in principle possible without any control that leads to a change in the system parameters. However, humans have sensors (e.g. muscle spindles, visual system) that definitely come into play. Due to the definition of 'self-stability' this seems to be an ostensible paradox. Therefore, we will first review the emergence of the term 'self-stability' in the literature. Then, we will try to reconcile the self-stability and the control approach.

Self-stability

To our knowledge the term 'self-stability' was introduced by Ringrose (Ringrose, 1997a; Ringrose, 1997b) in the field of robotics: 'Running motions can be self-stabilizing. That is, with proper design the structure and motion of a robot can automatically cause it to recover from minor disturbances even if it cannot detect them.' Recently, Blickhan and colleagues suggested how to identify self-stability in biological movement systems and to re-transfer these findings back to engineering (Blickhan et al., 2007). Before, these authors had integrated the term 'self-stability' into the framework of biomechanics (Blickhan et al., 2003). Accordingly, a biomechanical movement is called 'self-stable' if movement stability is gained by any flow of signals ('sensing' mechanical state variables) being exclusively coupled to forces. In dynamics, applying forces necessarily generates a flow of mechanical energy per time (power).

In other words, the forces acting on and within the movement system must exclusively depend on the mechanical state variables $\vec{\mathbf{x}}$ and the mechanical parameters (passive mechanics and actuators) $\{p_m\}$ of the movement system. Specific rheonomic constraints ['predetermined patterns' (Ringrose, 1997b)] $\vec{\mathbf{c}}(t,\{p_c\})$, i.e.

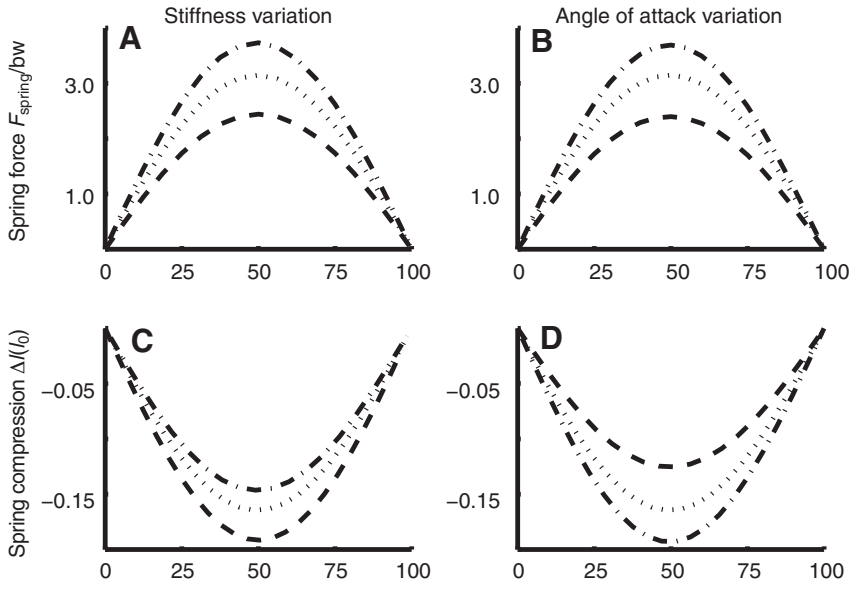

Fig. 7. Simulation results of peak spring force (F_{spring}) and maximum spring compression (Δl) for a 15 cm step in the second contact dependent on a variation of spring stiffness ($\tilde{k}$) and angle of attack (α_{TD}). All simulations started before the first contact on ground level with identical initial conditions ($v_{x,0}$=4.5 m s^{-1}, y_0=0.95 m) and system parameters ($\tilde{k}$=35.7, α_{TD}=68 deg., m=80 kg, l_0=1 m). (A,C) By using a fixed angle of attack and decreasing spring stiffness we found that spring force decreased while spring compression increased. Dash-dotted line, $\tilde{k}$=25.5, α_{TD}=61 deg.; dotted line $\tilde{k}$=19.1, α_{TD}=61 deg.; dashed line, $\tilde{k}$=12.7, α_{TD}=61 deg. (B,D) In the case of varying (steepening) the angle of attack and using a fixed spring stiffness, spring force and spring compression decreased. Dash-dotted line, α_{TD}=59 deg., $\tilde{k}$=19.1; dotted line, α_{TD}=61 deg., $\tilde{k}$=19.1; dashed line, α_{TD}=63 deg., $\tilde{k}$=19.1.

mechanical state variables, external or internal forces, muscle activations or stimulations exclusively and explicitly varying with time, can contribute to self-stable movement. Thus, the equations of motion have the form:

$$\dot{\vec{\mathbf{x}}} = \vec{\mathbf{f}}(\vec{\mathbf{c}}(t, \{p_c\}), \vec{\mathbf{x}}, \{p_m\}) ,$$

where the $\dot{\vec{\mathbf{x}}}$ denotes the first time derivative of the state and the parameters $\{p_c\}$ define the rheonomic constraints as an explicit function of time. In order to decide whether a parameter is of mechanical or non-mechanical (e.g. sensory feedback gain) character, one has to (i) mathematically formulate a model of the movement system and (ii) suggest a re-implementation of the model in the real world (e.g. prosthesis or robot). According to this definition, dissipative and thermodynamically open systems driven by internal or external energy sources may be as self-stable as closed conservative systems.

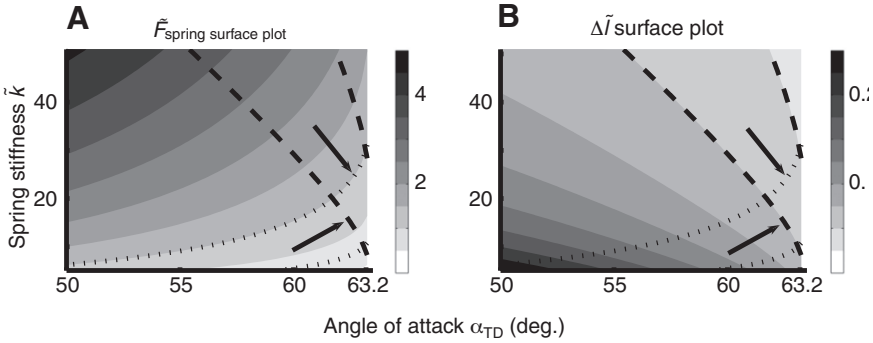

Fig. 8. Estimation of peak spring force and maximum spring compression in the case of a disturbed contact (15 cm step up) with a varied angle of attack and spring stiffness for a spring–mass simulation. The dotted lines indicate spring forces between 1.5 and 3 times gravitational force and the black lines indicate spring compressions between 0.1 and 0.15 times initial leg length. The arrows highlight the small areas of experimentally measured values. (A) In the simulation, decreasing spring stiffness and steepening angle of attack led to a decreasing peak spring force. (B) However, an increasing maximum spring compression with increasing spring stiffness can only be realized by substantially flattening the angle of attack. Initial conditions on ground level were $v_{x,0}$=4.5 m s^{-1}, y_0=0.95 m, m=80 kg, l_0=1 m, and were altered in the consecutive contact due to the step.

For example, a movement generated by a 'predetermined pattern' acting as input to a musculo-skeletal system under gravity (Ringrose, 1997b; Aoi and Tsuchiya, 2007) might be as self-stable as spring–mass walking (Geyer et al., 2006) or running (Seyfarth et al., 2002; Ghigliazza et al., 2005; Owaki and Ishiguro, 2007). Other examples of self-stable mechanisms are: a purely passive robot steadily moving down a slope under gravity plus roll friction (McGeer, 1990a; McGeer, 1990b), insect locomotion in the horizontal plane (Schmitt and Holmes, 2000a; Schmitt and Holmes, 2000b; Schmitt and Holmes, 2001), oscillations induced by a fixed muscle stimulation program (Wagner and Blickhan, 1999; Wagner and Blickhan, 2003), robot juggling (Schaal et al., 1996), and somersault locomotion (Mombaur et al., 2005).

To represent a 'predetermined pattern', a 'central pattern generator' (CPG) must fulfil the rheonomic requirement. This statement corresponds exactly to Full and Koditschek (Full and Koditschek, 1999): 'The Kubow and Full (1999) dynamic, cockroach model prescribes leg forces using a feedforward clock analogous to a central pattern generator with no equivalent of neural feedback among any of the components... The model self-stabilizes.' At first view, the sketched feedback arrow that the authors present in their illustration 3 (connecting sensors to CPG) seems to contradict their own CPG definition. Taking a closer look, the arrow might be interpreted as the option to transmit discrete bits of information (e.g. the event 'reset the clock' or, more generally, resetting a state variable) rather than to represent an intermittent or continuous flow of signals being used to change system parameters dependent on an error signal (feedback).

Note that the definition of 'self-stability' does not interfere with the specific approach (e.g. using 'Lyapunov-stability' or 'return-maps', or finding 'basins of attraction') chosen to quantify dynamic stability.

Reconciling self-stability and control

If all subsystems (e.g. muscles, neurons, joints, limbs) of a biological movement system [an 'anchor' (Full and Koditschek, 1999)] cooperate in order to generate behaviour represented by a model [a 'template' (Full and Koditschek, 1999)], the system benefits if self-stability is an inherent property of the model. With self-stability, the movement system gains energetic efficiency with increasing contributions of elastic parts. The system also gains control efficiency (reduced signal and information flow, in engineering the latter being equivalent to reduced 'bandwidth') as, according to the definition of self-stability, the system in principle would not need any continuous sensor signal flow of state variables, other than from mechanical dynamics, to generate the specific movement.

During stance phase the runner benefits from self-stability because his take-off conditions provide excellent touch-down conditions for the following contact phase. Neural signals may contribute to self-stability if they provide event detection [processed signals, i.e. information about loss of ground contact, 'reset the angle' (Ghigliazza et al., 2005)]. In contrast, continuous flow of neural signals by definition would not contribute to self-stability. However, it contributes to parameter tuning potentially supporting underlying self-stability (Wagner and Giesl, 2006). For example, non-linear characteristics on the joint level linearize the leg force–length relationship (Seyfarth et al., 1999; Günther and Blickhan, 2002). These non-linearities may come from leg segment geometry (Günther et al., 2004), tendon properties (Maganaris and Paul, 1999; Ker, 2007) or muscle–tendon complex properties (Seyfarth et al., 1999). On the other hand, neuro-muscular control mechanisms may linearize the muscle force–length relationship (Hoffer and Andreassen, 1978; Greene and McMahon, 1979; Hoffer and Andreassen, 1981; Maganaris, 2003).

Feedback can also be used to stabilize a movement system with an increased number of degrees of freedom still profiting from self-stability of a lower dimensional subsystem (Jindrich and Full, 2002; Seipel and Holmes, 2005; Seipel and Holmes, 2006). Furthermore, feedback can increase the robustness of a mechanical system against parameter variations and/or perturbations (Geyer et al., 2003; Schmitt and Holmes, 2003; Seipel and Holmes, 2007).

The simple spring–mass model is robust against small variations in angle of attack and very robust when leg retraction is applied (Seyfarth et al., 2003; Seyfarth et al., 2006). As mentioned above, the measured angle of attack accordingly decreases when step height increases, i.e. leg retraction is unaltered. Following Seyfarth (Seyfarth, 2002; Seyfarth, 2003), stiffness could be kept constant, whereas in the experiment, stiffness was reduced with increasing step height. It seems that during flight phase anticipatory influences become effective. The

runner predicts the perturbation and changes leg stiffness. This is feed-forward control. Feed-forward control requires prediction based on a model, whether implicit or explicit (A. J. Ijspeert, personal communication). For running, we suggest that the self-stabilizing spring–mass model is suitable. Then, if leg stiffness is adjusted to the expected angle of attack within the predicted stiffness-angle area of stability (J-shape, Fig. 6), the feed-forward control leads to a new self-stabilizing touch-down condition. As even the simplest spring–mass model allows for manifold self-stable solutions, the additional application of control (change of stiffness) can serve multiple movement goals. Control reduces the number of self-stable solutions. Though the cause of stiffness adaptation on uneven and compliant ground might be different, the movement target is the same. Besides stability, runners prefer a smooth ride of the centre of mass trajectory (Ferris et al., 1999). Blickhan and colleagues discussed a step-wise response to a disturbance and suggested that strong accelerations of the head following an abrupt alteration of the centre of mass are energetically detrimental (Blickhan et al., 2003).

By generating biological movements in accordance with the self-stable solutions of less complex movement systems, increasingly complex systems inherit the underlying stability. To achieve this, control strategies and structures have to be adjusted to the self-stable design of the less complex system (e.g. Cham et al., 2004).

APPENDIX

We want to calculate the eigenfrequency:

$$\omega_{\mathrm{d}} = \sqrt{\omega_0^2 - \gamma^2} \tag{A1}$$

of the damped harmonic oscillator:

$$m\Delta\ddot{l} + d\Delta\dot{l} + k\Delta l = 0 \tag{A2}$$

with $d=2m\gamma$ the damping coefficient, m the mass, k the stiffness, Δl the displacement, in terms of energy loss:

$$\Delta E = -\int_0^{2\pi/\omega_{\mathrm{d}}} 2m\gamma\Delta\dot{l}^2\mathrm{d}t = \int_0^{2\pi/\omega_{\mathrm{d}}} \frac{\mathrm{d}}{\mathrm{d}t}\left(\frac{1}{2}m\Delta\dot{l}^2 + \frac{1}{2}k\Delta l^2\right)\mathrm{d}t \tag{A3}$$

during one (damped) oscillatory period $T_d=2\pi/\omega_d$ and the undamped eigenfrequency:

$$\omega_0 = \sqrt{\frac{k}{m}} \quad . \tag{A4}$$

Note that $\Delta E<0$ for a damped system ($d>0$).

The solution of the dynamic equation of motion is:

$$\Delta l(t) = Ae^{-\gamma t}\sin(\omega_{\mathrm{d}}t + \delta) \tag{A5}$$

with t the time, A the amplitude and Δ the phase. To determine the relative energy loss $\Delta E/E$ during one period we assume the typical energy content of the oscillator to be estimated by the initial kinetic energy $E=\frac{1}{2}A^2m\omega_d^2$ (in the specific case $\delta=0$) or, equivalently, by the maximum stored elastic energy $E=\frac{1}{2}k\Delta l_{\mathrm{max}}^2$.

Therefore, using Eqn A5 the left integral in Eqn A3 solves to:

$$\Delta E / E = e^{-\frac{4\pi\gamma}{\omega_{\mathrm{d}}}} - 1$$

which can explicitly be resolved for:

$$\gamma^2 = \frac{\omega_d^2}{16\pi^2}\ln^2\left(\frac{1}{1+\Delta E/E}\right)$$

and, thus, Eqn A1 becomes:

$$\omega_d = \omega_0\sqrt{\frac{1}{1+\left(4\pi\ln\left(\frac{1}{1+\Delta E/E}\right)\right)^2}} \tag{A6}$$

as desired.

Taking only the first order term within the Taylor expansion of the ln-function in Eqn A6 into account results in:

$$\omega_d = \omega_0\sqrt{\frac{1}{1+(4\pi\Delta E/E)^2}} \tag{A7}$$

representing an approximation for small $\Delta E/E$.

From Eqn A7 we find the often-used quality factor $Q=-2\pi(E/\Delta E)=\omega_d/2\gamma$ and the linear damping coefficient $d=-(m\omega_d/2\pi)(\Delta E/E)=-(m/T_d)(\Delta E/E)$.

LIST OF ABBREVIATIONS

bw	body weight
E_{leg}	maximum energy stored in the axial leg spring, $E_{\mathrm{leg}}=\frac{1}{2}k_{\mathrm{leg}}\Delta l_{\mathrm{leg,max}}^2$
ΔE_{leg}	axial net energy balance of the leg, i.e. the area of the force–length work-loop: $\Delta E_{\mathrm{leg}} = \int_{l_{\mathrm{leg,TD}}}^{l_{\mathrm{leg,TO}}} F\mathrm{d}l_{\mathrm{leg}}$
$\Delta E_{\mathrm{leg}}/E_{\mathrm{leg}}$	relative energy balance
F_{max}	peak ground reaction force
$\tilde{F}_{\mathrm{max}}$	normalized peak ground reaction force in body weight (bw)
$\boldsymbol{g}$	gravitational acceleration
GRF	ground reaction force
$\tilde{k}$	dimensionless stiffness, symbol only used in simulation
k_{leg}	leg stiffness
$\tilde{k}_{\mathrm{leg}}$	dimensionless leg stiffness
l_0	initial leg length, i.e. the maximum length as a sum of all segments of the leg (static recorded)
l_{leg}	actual leg length (distance between hip and ball marker)
$\tilde{l}_{\mathrm{leg}}$	dimensionless leg length, leg length in terms of initial leg length. Indices are: TD, leg length at TD; TO, leg length at TO; shift, leg lengthening or shortening during contact
Δl_{leg}	leg compression
$\Delta\tilde{l}_{\mathrm{leg}}$	dimensionless leg compression
$\Delta l_{\mathrm{leg,max}}$	amount of maximum leg compression, i.e. difference between leg length at TD and minimum leg length during contact
$\Delta\tilde{l}_{\mathrm{leg,max}}$	dimensionless amount of maximum leg compression
m	body mass
t_{c}	contact time
$t_{\tilde{F}_{\mathrm{max}}}$	instant of peak force
$t_{\Delta\tilde{l}_{\mathrm{leg,max}}}$	instant of maximum leg compression
TD	touch-down, start of contact
TO	take-off, end of contact
v_x, v_y	horizontal (x) and vertical (y) component of the centre of mass velocity, in experimental data estimated from the velocity of the hip marker. Indices refer to points in time; here, TD and TO.
$v_{x,0}$	horizontal component of the initial velocity; only in simulation
y_0	initial apex height; only in simulation
α	leg angle, clockwise with respect to the negative x-axis with indices: TD, angle of attack (leg angle at TD); TO, leg angle at TO; shift, shift of leg angle from TD to TO
φ	joint angle, i.e. inner segmental angle for knee and ankle joint with indices: TD, joint angle at TD; TO, joint angle at TO; min, minimum joint angle during stance phase

We would like to thank Michelle Huth and James A. Smith for proof reading the manuscript, André Seyfarth for useful comments on the discussion, Tom Weihmann for his probing questions on self-stability, and Anne Liebetrau and Christian Rode for comments on the definition of self-stability. We also thank Hartmut Geyer for comments during the review process. The research was supported by grants from the 'Deutsche Forschungsgemeinschaft (DFG)' to M.E. (part of the current project 'Natur und Technik intelligenten Laufens': BL 236/15-2) and M.G. (MU 1766/1-2).

REFERENCES

Alexander, R. M. (1997). Invited editorial on 'interaction of leg stiffness and surface stiffness during human hopping'. *J. Appl. Physiol.* **82**, 13-14.
Aoi, S. and Tsuchiya, K. (2007). Self-stability of a simple walking model driven by a rhythmic signal. *Nonlinear Dynamics Psychol. Life Sci.* **48**, 16.
Biewener, A. A. (1989). Scaling body support in mammals: limb posture and muscle mechanics. *Science* **245**, 45-48.
Biewener, A. A. and Daley, M. A. (2007). Unsteady locomotion: integrating muscle function with whole body dynamics and neuromuscular control. *J. Exp. Biol.* **210**, 2949-2960.
Biewener, A. A., Farley, C. T., Roberts, T. J. and Temaner, M. (2004). Muscle mechanical advantage of human walking and running: implications for energy cost. *J. Appl. Physiol.* **97**, 2266-2274.
Blickhan, R. (1989). The spring-mass model for running and hopping. *J. Biomech.* **22**, 1217-1227.
Blickhan, R. and Full, R. J. (1993). Similarity in multilegged locomotion: Bouncing like a monopode. *J. Comp. Physiol. A: Neuroethol. Sens. Neural. Behav. Physiol.* **173**, 509-517.
Blickhan, R., Wagner, H. and Seyfarth, A. (2003). Brain or Muscles? In *Recent Research Developments in Biomechanics* **1** (ed. S. G. Pandalai), pp. 215-245. Thiru-anantha-puram (Trivandrum): Transworld Research Network.
Blickhan, R., Seyfarth, A., Geyer, H., Grimmer, S., Wagner, H. and Günther, M. (2007). Intelligence by mechanics. *Philos. Transact. A Math. Phys. Eng. Sci.* **365**, 199-220.
Brown, I. E., Scott, S. H. and Loeb, G. E. (1996). Mechanics of feline soleus: II design and validation of a mathematical model. *J. Muscle Res. Cell. Motil.* **17**, 221-233.
Cavanagh, P. R. and Lafortune, M. A. (1980). Ground reaction forces in distance running. *J. Biomech.* **13**, 397-406.
Cham, J. G., Karpick, J. K. and Cutkosky, M. R. (2004). Stride Period Adaptation of a Biomimetic Running Hexapod. *Int. J. Rob. Res.* **23**, 141-153.
Daley, M. A. and Biewener, A. A. (2006). Running over rough terrain reveals limb control for intrinsic stability. *Proc. Natl. Acad. Sci. USA* **103**, 15681-15686.
Daley, M. A., Usherwood, J. R., Felix, G. and Biewener, A. A. (2006). Running over rough terrain: guinea fowl maintain dynamic stability despite a large unexpected change in substrate height. *J. Exp. Biol.* **209**, 171-187.
de Wit, B., de Clercq, D. and Aerts, P. (2000). Biomechanical analysis of the stance phase during barefoot running. *J. Biomech.* **33**, 269-278.
Farley, C. T. and Gonzalez, O. (1996). Leg stiffness and stride frequency in human running. *J. Biomech.* **29**, 181-186.
Farley, C. T., Glasheen, J. and McMahon, T. A. (1993). Running springs: speed and animal size. *J. Exp. Biol.* **185**, 71-86.
Farley, C. T., Blickhan, R., Saito, J. and Taylor, C. R. (1991). Hopping frequency in humans: a test of how springs set stride frequency in bouncing gaits. *J. Appl. Physiol.* **71**, 2127-2132.
Farley, C. T., Houdijk, H. H., Van Strien, C. and Louie, M. (1998). Mechanism of leg stiffness adjustment for hopping on surfaces of different stiffnesses. *J. Appl. Physiol.* **85**, 1044-1055.
Ferris, D. P. and Farley, C. T. (1997). Interaction of leg stiffness and surfaces stiffness during human hopping. *J. Appl. Physiol.* **82**, 15-22.
Ferris, D. P., Louie, M. and Farley, C. T. (1998). Running in the real world: adjusting leg stiffness for different surfaces. *Proc. Biol. Sci.* **265**, 989-994.
Ferris, D. P., Liang, K. and Farley, C. T. (1999). Runners adjust leg stiffness for their first step on a new running surface. *J. Biomech.* **32**, 787-794.
Friedman, M. (1937). The use of ranks to avoid the assumption of normality implicit in the analysis of variance. *J. Am. Stat. Assoc.* **32** 675-701.
Friedman, M. (1939). A correction: the use of ranks to avoid the assumption of normality implicit in the analysis of variance. *J. Am. Stat. Assoc.* **34**, 109.
Full, R. J. and Koditschek, D. E. (1999). Templates and anchors: neuromechanical hypotheses of legged locomotion on land. *J. Exp. Biol.* **202**, 3325-3332.
Full, R. J., Kubow, T., Schmitt, J., Holmes, P. and Koditschek, D. (2002). Quantifying dynamic stability and maneuverability in legged locomotion. *Integr. Comp. Biol.* **42**, 149-157.
Geyer, H. (2005). Simple models of legged locomotion based on compliant limb behavior. PhD-Thesis, Friedrich-Schiller-Universität, Jena Germany, pp. 114.
Geyer, H., Blickhan, R. and Seyfarth, A. (2002). Natural dynamics of spring-like running: emergence of selfstability. In *5th International Conference on Climbing and Walking Robots* (ed. P. Bidaud and F. B. Amar). Paris: Professional Engineering Publishing.
Geyer, H., Seyfarth, A. and Blickhan, R. (2003). Positive force feedback in bouncing gaits? *Proc. Biol. Sci.* **270**, 2173-2183.
Geyer, H., Seyfarth, A. and Blickhan, R. (2005). Spring-mass running: simple approximate solution and application to gait stability. *J. Theor. Biol.* **232**, 315-328.
Geyer, H., Seyfarth, A. and Blickhan, R. (2006). Compliant leg behaviour explains basic dynamics of walking and running. *Proc. Biol. Sci.* **273**, 2861-2867.
Ghigliazza, R. M., Altendorfer, R., Holmes, P. and Koditschek, D. (2005). A simply stabilized running model. *J. Appl. Dyn. Sys.* **47**, 519-549.
Greene, P. R. and McMahon, T. A. (1979). Reflex stiffness of man's anti-gravity muscles during kneebends while carrying extra weights. *J. Biomech.* **12**, 881-891.
Günther, M. and Blickhan, R. (2002). Joint stiffness of the ankle and the knee in running. *J. Biomech.* **35**, 1459-1474.
Günther, M., Sholukha, V. A., Kessler, D., Wank, V. and Blickhan, R. (2003). Dealing with skin motion and wobbling masses in inverse dynamics. *J. Mech. Med. Biol.* **3**, 309-335.
Günther, M., Keppler, V., Seyfarth, A. and Blickhan, R. (2004). Human leg design: optimal axial alignment under constraints. *J. Math. Biol.* **48**, 623-646.
Hoffer, J. A. and Andreassen, S. (1978). Factors affecting the gain of the stretch reflex and soleus muscle stiffness in premammillary cats. *Soc. Neurosci.* **4**, 935.
Hoffer, J. A. and Andreassen, S. (1981). Regulation of soleus muscle stiffness in premammillary cats: intrinsic and reflex components. *J. Neurophysiol.* **45**, 267-285.
Jindrich, D. L. and Full, R. (2002). Dynamic stabilization of rapid hexapedal locomotion. *J. Exp. Biol.* **205**, 2803-2823.
Ker, R. F. (2007). Mechanics of tendon, from an engineering perspective. *Int. J. Fatigue* **29**, 1001-1009.
Kerdok, A. E., Biewener, A. A., McMahon, T. A., Weyand, P. G. and Herr, H. M. (2002). Energetics and mechanics of human running on surfaces of different stiffnesses. *J. Appl. Physiol.* **92**, 469-478.
Kubow, T. M. and Full, R. J. (1999). The role of the mechanical system in control: a hypothesis of self-stabilization in hexapedal runners. *Philos. Trans. R. Soc. Lond., B, Biol. Sci.* **354**, 849-861.
Lindstedt, S. (2003). Springs in legs and running surfaces. *J. Exp. Biol.* **206**, 8.
Maganaris, C. N. (2003). Force-length characteristics of the in vivo human gastrocnemius muscle. *Clin. Anat.* **16**, 215-223.
Maganaris, C. N. and Paul, J. P. (1999). In vivo human tendon mechanical properties. *J. Physiol.* **521**, 307-313.
McGeer, T. (1990a). Passive bipedal running. *Proc. R. Soc. Lond., B, Biol. Sci.* **240**, 107-134.
McGeer, T. (1990b). Passive Dynamic Walking. *Int. J. Rob. Res.* **9**, 62-82.
McMahon, T. A. and Cheng, G. C. (1990). The mechanics of running: how does stiffness couple with speed. *J. Biomech.* **23**, 65-78.
Mombaur, K. D., Bock, H. G., Schloder, J. P. and Longman, R. W. (2005). Self-stabilizing somersaults. *IEEE Trans. Rob. Autom.* **21**, 1148-1157.
Moritz, C. T. and Farley, C. T. (2004). Passive dynamics change leg mechanics for an unexpected surface during human hopping. *J. Appl. Physiol.* **97**, 1313-1322.
Owaki, D. and Ishiguro, A. (2007). Mechanical dynamics that enables stable passive dynamic bipedal running – Enhancing self-stability by exploiting nonlinearity in the leg elasticity. *J. Rob. Mech.* **19**, 374-380.
Patla, A. E. and Rietdyk, S. (1993). Visual control of limb trajectory over obstacles during locomotion effect of obstacle height and width. *Gait Posture* **1**, 45-60.
Ringrose, R. P. (1997a). Self-stabilizing robot. *Proceedings of {IEEE} International Conference on Robotics and Automation* **1**, 487-493.
Ringrose, R. P. (1997b). Self-stabilizing running., PhD-Thesis, pp. 131. Boston: Massachusetts Institute of Technology.
Schaal, S., Atkeson, C. and Sternad, D. (1996). One-handed juggling: A dynamical approach to a rhythmic movement task. *J. Mot. Behav.* **28**, 165-183.
Schmitt, J. and Holmes, P. (2000a). Mechanical models for insect locomotion: dynamics and stability in the horizontal plane I. Theory. *Biol. Cybern.* **83**, 501-515.
Schmitt, J. and Holmes, P. (2000b). Mechanical models for insect locomotion: dynamics and stability in the horizontal plane-II. Application. *Biol. Cybern.* **83**, 517-527.
Schmitt, J. and Holmes, P. (2001). Mechanical models for insect locomotion: stability and parameter studies. *Physica D: Nonlinear Phenomena* **156**, 139-168.
Schmitt, J. and Holmes, P. (2003). Mechanical models for insect locomotion: active muscles and energy losses. *Biol. Cybern.* **89**, 43-55.
Schmitt, J., Garcia, M., Razo, R. C., Holmes, P. and Full, R. J. (2002). Dynamics and stability of legged locomotion in the horizontal plane: a test case using insects. *Biol. Cybern.* **86**, 343-353.
Seipel, J. and Holmes, P. (2005). Running in three dimensions: analysis of a point-mass sprung-leg model. *Int. J. Rob. Res.* **24**, 657-674.
Seipel, J. and Holmes, P. (2006). Three-dimensional translational dynamics and stability of multi-legged runners. *Int. J. Rob. Res.* **25**, 889-902.
Seipel, J. and Holmes, P. (2007). A simple model for clock-actuated legged locomotion. *Reg. Chao. Dyn.* **12**, 502-520.
Seyfarth, A. (2000). Elastically operating legs-strategies and construction principles. PhD-Thesis, Friedrich-Schiller-Universität, Jena, Germany, pp. 108.
Seyfarth, A., Friedrichs, A., Wank, V. and Blickhan, R. (1999). Dynamics of the long jump. *J. Biomech.* **32**, 1259-1267.
Seyfarth, A., Geyer, H., Günther, M. and Blickhan, R. (2002). A movement criterion for running. *J. Biomech.* **35**, 649-655.
Seyfarth, A., Geyer, H. and Herr, H. (2003). Swing-leg retraction: a simple control model for stable running. *J. Exp. Biol.* **206**, 2547-2555.
Seyfarth, A., Geyer, H., Blickhan, R., Lipfert, S., Rummel, J., Minekawa, Y. and Iida, F. (2006). Running and walking with compliant legs. In *Fast Motions in Biomechanics and Robotics – Optimization and Feedback Control* (ed. M. Diehl and K. Mombaur), pp. 383-402. Berlin, Heidelberg: Springer.
Siegel, S. and Castellan, N. J. J. (1988). *Nonparametric Statistics for the Behavioral Sciences*. New York: McGraw-Hill.
Wagner, H. and Blickhan, R. (1999). Stabilizing function of skeletal muscles: an analytical investigation. *J. Theor. Biol.* **199**, 163-179.
Wagner, H. and Blickhan, R. (2003). Stabilizing function of antagonistic neuromusculoskeletal systems: an analytical investigation. *Biol. Cybern.* **89**, 71-79.
Wagner, H. and Giesl, P. (2006). Self-stability in Biological Systems-Studies based on Biomechanical Models. In *Fast Motions in Biomechanics and Robotics: Optimization and Feedback Control* (ed. M. Diehl and K. Mombaur), pp. 403-410. Berlin, Heidelberg: Springer.
Winter, D. A. (2005). *Biomechanics and Motor Control of Human Movement*. Hoboken, NJ: John Wiley.